An optimized radial basis function model for color characterization of a mobile device display

Ante Poljicak[a,*], Jurica Dolic[a], Jesenka Pibernik[a]

[a]*University of Zagreb, Faculty of Graphic Arts, Getaldiceva 2, Zagreb, Croatia*

Abstract

This paper presents an optimized color characterization model based on radial basis functions (RBF). The performance of the proposed model was tested on a number of different mobile devices and compared with the performance of other state of the art color characterization models. We compared the accuracy of models using the CIELAB color difference. Four different models were discussed in detail: Piecewise Linear Model Assuming Variation in Chromaticity, Polynomial regression, Artificial Neural Network, and proposed Radial Basis Function model. For training and evaluation of the models we measured a large number of color samples on various mobile device displays. Results have shown that our optimized RBF model has superior accuracy over other models with median color difference of 0.39. In addition, it has particularly good accuracy for colors on the boundary of device's gamut with maximum color difference of 0.87, where other models shown unacceptably high (>10) color difference.

Keywords: Approximation methods, Characterization, Colorimetry, Color Displays, Neural Networks, Piecewise linear approximation, Radial Basis Functions

2010 MSC: 00-01, 99-00

---

*Corresponding author

Email addresses: ante.poljicak@grf.hr (Ante Poljicak), jurica.dolic@grf.hr (Jurica Dolic), jesenka.pibernik@grf.hr (Jesenka Pibernik)

1. Introduction

Mobile devices today are ubiquitous and used in wide range of different applications from personal communication to image reproduction. Equipped with powerful imaging and processing hardware, mobile devices enable users to capture and view high resolution static images and interactive content. The expanding functionality of mobile devices is followed by rapid development of transmissive and emissive mobile display technologies.

Most mobile devices on the market feature an Active Matrix Liquid Crystal Display (AMLCD) or an Active Matrix Organic Light-Emitting diode (AMOLED) display. AMLCD is a transmissive display technology based on controlled orientation of molecules in the liquid crystal (LC) layer through which light passes and forms the rendered image on the display. The LC layer is situated between two electrodes, one being controlled by active-matrix backplane and the other situated beneath the colour filter. By controlling the voltage difference between the electrodes, molecular array of liquid crystals can be adjusted, thus controlling the intensity of the transmitted light [1]. Several different configurations of molecules in the LC layer, or Liquid Crystal Display Modes, exist: Twisted-Nematic (TN), In-Plane Switching (IPS), Vertical Alignment (VA) and Patterned Vertical Alignment (PVA). AMOLED represents an emissive display technology. AMOLED panels consist of series of organic thin films situated between two electrodes, a metal-based cathode and transparent anode. Instead of usual RGB subpixel array, AMOLED displays found in mobile devices often feature a RG-BG subpixel array, also known as PenTile array [2]. Compared to AMLCDs, AMOLEDs usually offer wider-viewing angles, better contrast ratio, significantly wider gamut and thinner construction, which make this technology attractive for mobile displays.

The progress and widespread use of mobile technology is not adequately followed by research on colorimetric characterization of mobile devices. The display characterization in general is extensively researched. Authors in [3, 4, 5] give an extended overview of methods for characterizing CRT displays.

2

While methods for characterization of LCD displays is given in [6, 7, 8]. On the other hand research on characterization focused just on mobile displays is very limited. Only Piecewise Linear Model Assuming Constant Chromaticity (PLCC), Piecewise Linear Model Assuming Variation in Chromaticity (PLVC), and masking models where applied on mobile device diplays [9].

The goal of our paper is to broaden the available research on the subject of color characterization of mobile device displays, and to develop flexible and accurate model for color characterization of mobile device display. We propose a model for color characterization of mobile device display based on Radial Basis Functions (RBF) and compare its performance against other popular approaches for color characterization: Piecewise Linear Model Assuming Variation in Chromaticity (PLVC), Polynomial Regression model, Artificial Neural Network (ANN) model. We compare performance of the models in respect to number of training samples needed and color difference between estimated and measured data. For training and evaluation we use data obtained from twenty different mobile devices with different AMLCD and AMOLED display technologies.

2. Theoretical

The main goal of the colorimetric characterization of a device is to obtain a model that will accurately transform color information from device dependent color space to device independent color space and vice versa. With the obtained model it is possible to estimate exact driving signals of the device for a needed color. A device dependent color space such are RGB and CMYK color spaces are not absolute color spaces, i.e. they differ from device to device. A device independent color space such are CIEXYZ and CIELAB are absolute and describe color as it is seen by a CIE standard observer [10]. In literature X, Y and Z values of CIEXYZ color space are also known as CIE tristimulus values.

According to [11] all methods or models can be classified in three different groups: the methods that try to physically model the behavior of a color device,

3

the methods based on numerical models, and the methods that are using 3D Look Up Tables (3D LUT).

Physical modeling is usually carried out in three steps. Firstly, the linearization of the tone reproduction curves (TRCs) of the devices' channels is done by modeling curves with a gamma law (CRT) or S-shaped curves (LCD) [12, 13, 14, 15, 16, 17]. When the signals are linearized, transformation from device dependent color space (RGB) to the device independent color space (CIEXYZ) is done. Finally, an offset is added to the output (1).

$$\mathbf{i} = \mathbf{M} \cdot f(\mathbf{d}) + \mathbf{o} \qquad (1)$$

Where, $\mathbf{i}$ denotes output vector in independent color space; d denotes vector with driving signals in dependent color space, $f(\cdot)$ is linearization function; $\mathbf{M}$ represent transformation matrix, while $\mathbf{o}$ denotes offset vector.

Generally, physical models assume a number of simplifying conditions such are channel independence, chromaticity constancy, spatial uniformity, and angle view independence. Channel independence assumes that the primaries of the device operate independently from one another. Chromaticity constancy assumes that each primary has constant chromaticity values regardless of the intensity of a driver signal. Spatial uniformity ensures that the output values will be the same, irrespective of the position on the device. Angle view independence assumes constant output values indifferent to the viewing angle. Color characterization of CRT displays was extensively studied in the past [18, 19, 20, 12, 4, 21] and this assumptions where tested and validated in experiments [18, 22].

Numerical characterization estimate transformation from a device dependent space to a device independent space using a numerical model. This model can be based on a number of different methods such as polynomial regression of n-th degree [23], neural networks [24, 25], sequential linear interpolation [26], or Radial Basis Functions (RBFs) [27, 28]. In comparison with the physical models, this approach is able to successfully model devices without assumption of channel independence. However, for this to be possible, large number of mea-

4

surement is needed. It should be noted that numerical methods are extensively used for characterization of printers as well [6, 29]

3D LUT models are based on tables with the information how to translate color information from a device dependent space to a device independent space. The accuracy of the model depends on the number of measurements taken to create the table [30], and the interpolation method to transform the color information for data that is between measurement points [31]. The main disadvantage of this approach is the need for large number of measurements. On the other hand, its advantage is that this approach does not imply any assumptions regarding the display technology.

2.1. Piecewise Linear Model Assuming Variation in Chromaticity

PLVC model was first proposed in 1980 by Farley and Gutmann in [32]. Later it was extensively used and evaluated for CRT displays [12, 33, 5], and for LCD displays [7, 6, 34]. It is extension of Piecewise linear model assuming constant chromaticity (PLCC), which it supersedes in accuracy, especially for displays where the chromaticity shift for different illuminance levels is high [11].

According to PLVC model, tristimulus values for any driving signal of the device can be expressed as a sum of tristimulus values for each primary for that driving signal. PLVC model can be generalized for any number of primaries, as well as for any number of possible levels of a driving signal. For a device with N primaries with L possible driving signal levels PLVC model is defined in (2).

$$X(p_1(s_1), p_2(s_2), \ldots, p_N(s_N)) = \sum_{i=1}^{i=N} [X(p_i(s_i)) - X_k] + X_k$$

$$Y(p_1(s_1), p_2(s_2), \ldots, p_N(s_N)) = \sum_{i=1}^{i=N} [Y(p_i(s_i)) - Y_k] + Y_k \qquad (2)$$

$$Z(p_1(s_1), p_2(s_2), \ldots, p_N(s_N)) = \sum_{i=1}^{i=N} [Z(p_i(s_i)) - Z_k] + Z_k$$

Where X, Y, Z denote CIE tristimulus values; p_i is i^{th} primary ($i \in [0, N]$) and s_i is a driving signal level for i^{th} primary ($s_i \in [0, L]$). X_k, Y_k, Z_k denote tristimulus values for black level, (i.e. $s_i = 0 \ \forall \ p_i$).

5

Since the values of the black level are included in every measured sample it is important to subtract it first from all samples, and then add it only once to ensure correct standard observer color space [35].

Main advantage of PLVC model is that it needs only a small number of measured samples. In addition it is very simple for the implementation. On the other hand, this model does not take into account channel interdependence.

Implementation of PLVC was done using (2) for $N = 3$ primaries (i.e. R, G and B). Nine different driving signals of each primary were used for the model (Sr, Sg, $Sb \ \epsilon \ [0, 32, 64, 96, 128, 160, 192, 224, 255]$). To calculate response of the model for other driving signals linear interpolation was used to as this approach was used in previously published research [7, 6, 34]. Note that the interpolation method can influence the performance of PLVC, however, this is not within the scope of this paper.

2.2. Polynomial Regression models

Regression models are statistical models used for estimation of relationships among variables. These well-known methods are used in wide range of applications from data fitting to data prediction. Many different regression methods exist such as linear, polynomial, robust, Bayesian, non-parametric, etc.

Polynomial regression is type of linear regression where the relationships between variables are modeled as n-th degree polynomial. It is often used to model complex nonlinear systems such as optical character recognition [36], multimodal biometrics classification [37], and color characterization [38, 39]. General n-th degree polynomial regression model using matrix notation is defined as (3).

$$\mathbf{y} = \mathbf{x} \cdot \mathbf{a} + \boldsymbol{\varepsilon} \qquad (3)$$

Where $\mathbf{y}$ denotes response vector, $\mathbf{a}$ parameter vector, $\boldsymbol{\varepsilon}$ random error vector, while $\mathbf{x}$ is vector containing independent variables.

6

Solution of the model in (3) is then given by the well-known normal equation [40]:

$$\mathbf{a} = (\mathbf{x^T x})^{-1}\mathbf{x^T y} \tag{4}$$

Equation (3) is an example of multidimensional polynomial regression model that is easy to use for multidimensional problem like color characterization of a color device. This approach can successfully take into account channel interdependence by using cross components factors in the model [4, 21, 34]. This is done by including in vector $\mathbf{x}$ products of driving signals for two or more primaries of a device. Excellent introduction to polynomial regression used for color characterization is given by Kang [41]. In our investigation, two different degrees of regression models were used: Polynomial regression of 2nd degree and polynomial regression of 3rd degree. Polynomial regression of 2nd degree has vector $\mathbf{x}$ with nine interdependent variables (5).

$$\mathbf{x} = [1\ r\ g\ b\ rg\ rb\ gb\ r^2\ g^2\ b^2] \tag{5}$$

This model takes into account channel interdependence for any two primaries (i.e. r, g, b). However, it is not able to model channel interaction for all three primaries. On the other hand, polynomial regression of 3rd degree has 19 variables capable of modeling channel interdependence for all three primaries (6).

$$\mathbf{x} = [1\ r\ g\ b\ rg\ rb\ gb\ r^2\ g^2\ b^2\ r^2g\ r^2b\ \ldots \\ g^2r\ g^2b\ b^2r\ b^2g\ r^3\ g^3\ b^3\ rgb] \tag{6}$$

2.3. Artificial Neural Networks

The artificial neural network (ANN) is model that simulates biological nervous system where each neuron of the ANN is analogue to nerve cell, and connections between neurons are analogue to synapses. An artificial neuron is

7
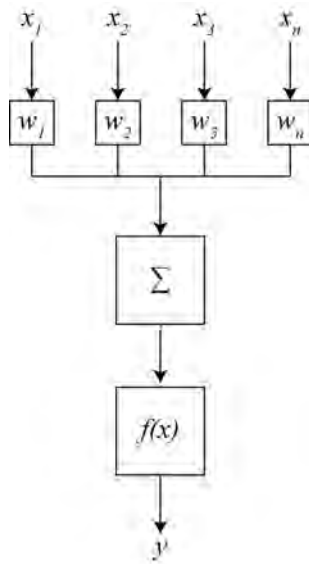
Fig. 1: Artificial neuron with inputs x_i, weights wi, transfer function $\sum$, activation function $f(x)$, and output y.

composed of three parts, inputs with weights, a transfer function and an activation function (Fig. 1). The transfer function usually adds together values from the weighted inputs, while activation function defines the output of the neuron: There are many types of activation functions used (e.g. identity, step, ramp, logistic) and the type of an activation function influence the behavior of the entire ANN.

The most important property of ANN is its ability to adaptively change the weights in artificial neurons to approximate the intrinsic properties of complex training data and to generalize this learnt properties for similar data not used in the training process. ANN is often used to process complex data in applications such as classification [42] or approximation [43]. Main advantage of ANNs is ability to adjust to data without any information regarding the process to be modeled. In addition, ANNs are nonlinear in nature and, therefore, capable to model very complex processes. Finally, they are capable to approximate any function with arbitrary accuracy [44]. However, it should be noted that the

8

accuracy of ANN is still limited with the size of the network and the availability of the data used in training [42]. Furthermore, ANNs are highly nonlinear in parameters which implies the use of nonlinear optimization techniques [45]. Other common problem with ANNs is over-fitting, where the network fits training data well but fails to generalize, i.e., fit data not used for training.

For an ANN architecture we used a simple network with input and output layers and one hidden layer. In the hidden layer as activation function we used logistic function while for the output layer linear function was used. For learning, the ANN model used Levenberg-Marquardt algorithm (LMA). Even though LMA is both time and memory consuming especially if the network has significant number of adaptive weights, it is very popular and often used for training of neural networks [46].

The architecture of the ANN model used in the experiment is show in Fig. 2. The number of neurons in input and output layers was fixed to three neurons. While the number of neurons in hidden layer was changed in order to find an optimal number of neurons.

3. Proposed model

We propose a new model based on Radial Basis Function (RBF) methods. It extends the work of Sharma and Shaw [27] and Colantoni et al. [28]. Authors in [27] proposed the use of thin-plate splines function $\theta(r) = r^2 \ln(r)$ for color characterization of a printer and thoroughly investigated the influence of size of the training data on the performance of the model. They concluded that this approach is fairly accurate when enough of data points is used for the training of the model. Authors in [28] extended existing research by utilizing additional basis functions, namely biharmonic $\theta(r) = r$, and triharmonic $\theta(r) = r^3$ and applied their model on CRT and LCD displays.

In our paper we further the investigation of RBFs by utilizing polyharmonic splines (8) with different k, Gaussian (9) and multiquadric (10) kernels. We investigate how this model performs in color characterization of a number of

9
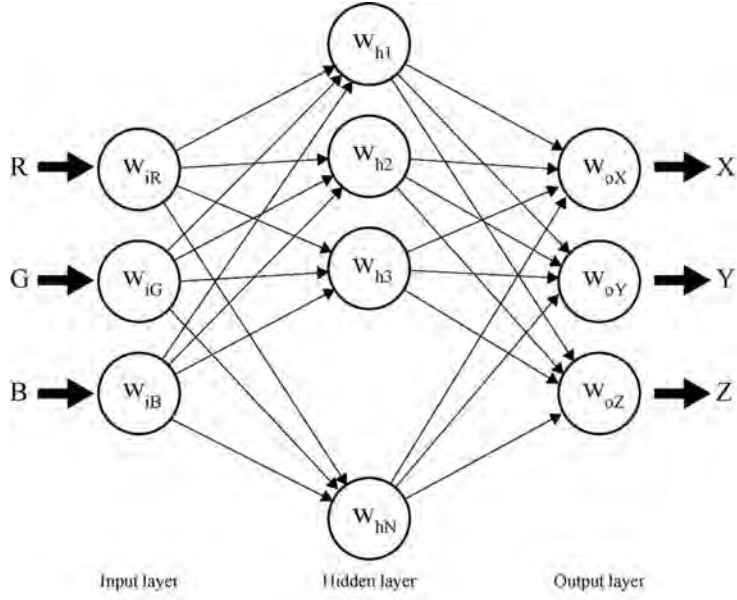
Fig. 2: Architecture of implemented ANN model with an input, hidden and output layer.

mobile devices, and optimize it by choosing the RBF kernel $\theta(\cdot)$ and modifying the scaling factor ε (7). After the optimization of the model we compare its performance against the performance of already mentioned models (i.e. PLVC, ANN, and polynomial regression).

One other important difference from previous research is that our model don't use smoothing factor used to overcome the problems of the display temporal stability. Reason why we have discarded this approach is that smoothing factor complicates the model, and our empirical data showed that repeatability between consecutive measurements of mobile device due to temporal variability was very small ($\Delta E_{ab}^* < 0.01$).

RBF methods are global interpolation methods proposed in [47] and revisited in [48]. The basic idea of RBF interpolation is to choose appropriate function $\theta(\cdot)$ (also known as kernel), and determine weights w_i depending on given data

points (7).

$$f(x) = \sum w_i \, \theta \|r_i\| \tag{7}$$

Where $f(x)$ is interpolated value at the point x, r_i denotes distance between given data point x_i to x (i.e. $r_i = x - x_i$). $\|\cdot\|$ is the Euclidean norm.

The choice of function $\theta(\cdot)$ should be made depending on the class of interpolation problem [31, 49]. Some of the kernels used are harmonic, multiquadric, Gaussian and polyharmonic splines.

The main advantage of RBF method is that it works well even if the data points on which fitting is based are scarce or unevenly distributed [49]. This is indeed the case for many applications especially when one wants to optimize a characterization procedure of a color device using as few data points as possible. We implemented RBF network using different kernels $\theta(\cdot)$, namely, polyharmonic splines of different order (8), gaussian (9) and multiquadric (10).

$$\theta(r) = \begin{cases} r^k & \text{for} \quad k = 1, 3, 5 \ldots \\ r^k \log(r) & \text{for} \quad k = 2, 4, 6 \ldots \end{cases} \tag{8}$$

$$\theta(r) = e^{-(\varepsilon r)^2} \tag{9}$$

$$\theta(r) = \sqrt{1 + (\varepsilon r)^2} \tag{10}$$

Note that scaling constant ε has impact on the overall performance of the model, especially for Gaussian. We have empirically found that optimal value for ε is from 2 to 5. In experiments we used $\varepsilon=3$.

After RBF function is chosen, weights w_i needed for model are then determined by using already mentioned normal equation [40]:

$$\mathbf{w} = (\boldsymbol{\theta}^{\mathbf{T}}\boldsymbol{\theta})^{-1}\boldsymbol{\theta}^{\mathbf{T}}\mathbf{x} \tag{11}$$

Where $\mathbf{w}$, $\boldsymbol{\theta}$ and $\mathbf{x}$ denote matrices of weights w_i, coefficients $\theta(r_i)$, and given data points x_i respectively.
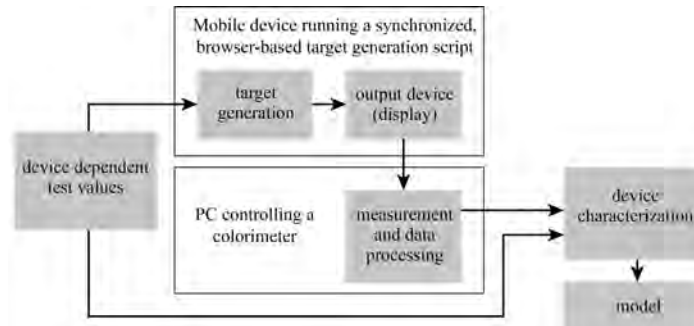
Fig. 3: Block diagram of the experimental setup used for measurement of a device color response and the training of models.

4. Experimental Setup

Experimental setup is shown in Fig. 3. Device dependent values in RGB space were sent to a mobile device using web based script. Response of the mobile device is then measured with luminance and color meter connected to a computer. Finally, measurements and device dependent values are used for training of models.

4.1. Measurement

For data acquisition we used 20 different mobile devices from various manufacturers and with different display technologies[1]. For each device 729 uniformly spaced color samples (i.e. different RGB combinations) were measured from black (RGB=0,0,0) to white (RGB=255,255,255). To avoid possible changes in brightness level during measurement, all devices were set to have fixed maximum brightness.

All measurements were done in CIEXYZ color space. Measuring distance from the device was 350 mm $\pm$ 1 mm, and angle from the normal was $0° \pm 0.5°$. Measurements were taken in completely dark room (illuminance $E < 10^{-4}$ lx). For measurement we used Konica Minolta CS-200 luminance and color meter

---

[1]Measurements can be downloaded from: `http://repro.grf.unizg.hr/media/Measurements_displays.zip`

with following parameters: Measurement time 2 s, Viewing angle 2°. To avoid possible errors due to instability of the device's display, each color sample was measured two times and mean was calculated. Distance from the display and viewing angle give measuring area $A_m = 117.25$ mm^2. With fixed measuring area the number of pixels measured depended only on spatial resolution of device (e.g. for the resolution of 10 px/mm the number of pixels measured is 11725). This large number of pixels, and the focus of measuring device set to infinity, minimizes the possibility of the influence of pixel variations on measurements.

After acquisition measured data was than uniformly divided in two subsets, a training subset used for training of the models, and the evaluation subset used for performance evaluation. Therefore, for training of models 365 equally spaced samples were used, while for evaluation 364 samples were used. Note that for PLVC model only 27 samples were used (nine for each primary).

4.2. Data preparation

As already mentioned, to avoid the influence of the different brightness between devices all displays have been set to their maximum brightness settings. This, however, still results in very different lightness values for different devices. These large differences are due to different technologies displays are using. We can neutralize this difference in measured lightness across devices by normalization of all measured values according to its maximum value for a given device (12):

$$Y_i' = \frac{Y_i}{Y_{max}} \tag{12}$$

Where Y_i' denotes normalized Y value in CIEXYZ color space; Y_i is measured Y value, and Y_{max} maximum Y value of all measurements of a given device.

4.3. Evaluation of a Model accuracy

To evaluate the accuracy of a model obtained results and measured evaluation samples were converted from CIEXYZ color space to more convenient CIELAB color space. As a white point needed for the conversion from CIEXYZ

13

to CIELAB color space, standard illuminant CIE D65 was used. We choose this illuminant as a white point since most LCD displays white point is near this illuminant [6], and it is recommended by CIE to be used for all colorimetric calculations requiring representative daylight illuminant [50]. However, note that the choice of the illuminant, if used consistently, will not influence the colorimetric comparison. For quantification of the color rendering accuracy of models, CIELAB color difference system was used. Color difference ΔE_{ab}^* is defined in (13). It is the Euclidean distance of two respective colors in CIELAB color space.

$$\Delta E_{ab}^* = \sqrt{(\Delta L^*)^2 + (\Delta a^*)^2 + (\Delta b^*)^2} \tag{13}$$

Where ΔL^*, Δa^* and Δb^* denote difference between respective colors in CIELAB color space for lightness axis (L^*) and two chromatic axis (a^*, b^*).

5. Results

The results were obtained by calculating ΔE_{ab}^* between measured values of evaluation colors and values estimated by a model. Calculation was done for all evaluation color samples and for each device. Results were then averaged according to (14).

$$\Delta E_{ab}^*{}^j = \frac{1}{N} \sum_{i=1}^{N} x_i^j \tag{14}$$

Where i denotes i-th device; j denotes j-th test color sample; x_i^j is color difference for given color sample and device; and N is total number of measured devices.

Before comparison of accuracy of all models, ANN and RBF models were first tested using different settings to find an optimum regarding accuracy and computational costs. For the ANN model we optimized the number of neurons in the hidden layer, while for RBF model we used different basis functions $\Theta(\cdot)$.
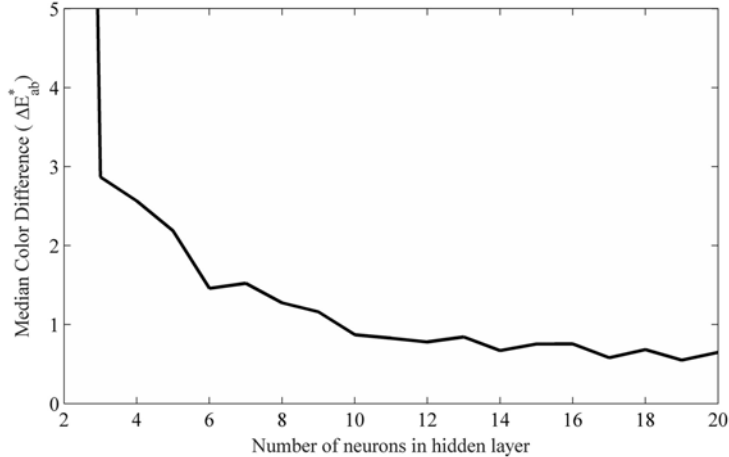
Fig. 4: Influence of the number of neurons in the hidden layer of ANN on the performance of the model. Diagram shows that an increase of number of nodes improves accuracy of the model. However, after 17 nodes there is no more improvement.

5.1. Model optimization

In ANN model the number of neurons in the network directly influences capability of modeling and complexity of implementation. This is confirmed in our experiment. As one can see in Fig. 4 the number of neurons in hidden layer of an ANN has strong impact on ΔE_{ab}^*. If the number of neurons is insufficiently small (i.e. less than six), the ANN model is not able to accurately characterize a display. An increase of the number of neurons improves the accuracy of the model. However, for the number of neurons reaches 17 there is no more improvement and accuracy remains the same.

To optimize RBF model for a function $\Theta(\cdot)$, we first used polyharmonic spline (8) with different k. We have shown that depending on the order k of polyharmonic spline, RBF model will have different performance. We calculated the accuracy for various k and found that the optimal value for k is 4. When this value is used RBF model has mean $\Delta E_{ab}^* = 0.46$ and median $\Delta E_{ab}^* = 0.39$. This order shows slightly better results than $k = 3$ which can also be used. Other orders have lower accuracy (Fig. 5). Note that authors in [28] report worse results of triharmonic kernel ($k = 3$) for two LCD devices they tested

15
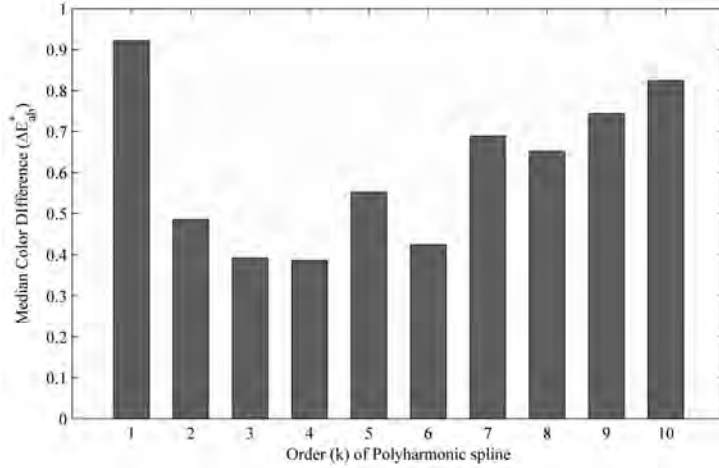
Fig. 5: Influence of order of the Polyharmonic spline on performance of the RBF model. Median ΔE_{ab}^* is lowest for $k = 4$.

(mean $\Delta E_{ab}^* = 0.783$ and 0.956).

When we found optimal order for polyharmonic spline we further our analysis by comparison of the accuracy of the RBF models that are using different basis functions $\Theta(\cdot)$. Fig. 6 shows that for the task of display characterization, polyharmonic spline (with $k = 4$) and multiquadric have almost the same accuracy, while accuracy of RBF with Gaussian is slightly worse. Median ΔE_{ab}^* values for polyharmonic ($k = 4$), Gaussian and multiquadric functions were 0.39, 0.49 and 0.41 respectfully.

5.2. Accuracy vs Number of Training Samples

Performance of a model and its usability for modeling depends on a number of training samples needed for accurate modeling. PLVC is in this respect in advantage over other models since it needs only a few measurements. Other models need larger set of training samples. To determine an optimal size of training set changed number of training samples and calculated the accuracy of models. Results of this investigation are shown in Fig. 7 and Fig. 8 Optimal number of training set for ANN and RBF model is around 150, while for polynomial regression of 3rd degree is around 100. Note that an increase of training set

16
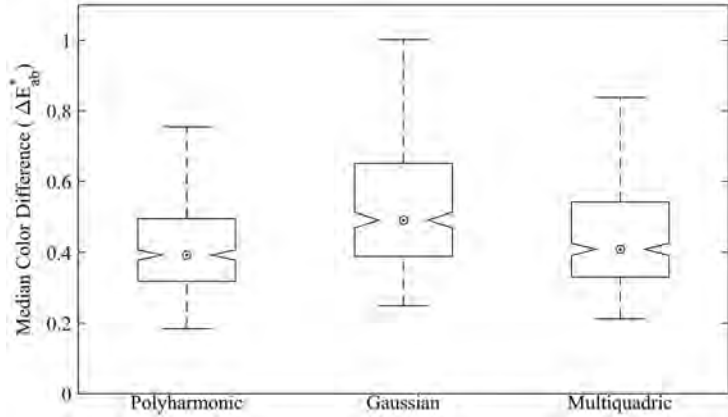
Fig. 6: Accuracy of RBF models using different functions. Polyharmonic spline with $k = 4$ have slightly better results than Gaussian or multiquadric.

sizes above mentioned optimal values have very little impact on median ΔE_{ab}^*. Nevertheless, when choosing the size of training set caution should be taken since with reduction of training samples, all models showed a strong increase in error for 95 percentile ΔE_{ab}^* (Fig. 8). This fact implies that larger number

340   of training samples can ensure better accuracy for extreme colors that are at the boundary of device's gamut (e.g. pure primaries and combinations of pure primaries). We also conducted this comparison for RBF models using different functions and found that RBF with Multiquadric function have better accuracy for low number of samples (<50) then with other functions. However, with 95

345   Percentile $\Delta E_{ab}^* > 20$, this fact have little practical importance.

5.3. Comparison of models

Finally, with optimized models, we proceed with the comparison of accuracy for all models. The results are given in Table 1 and illustrated in informative boxplot on Fig. 9. RBF model with Polyharmonic spline of order $k = 4$ showed

350   superior performance when compared to other models. With median ΔE_{ab}^* = 0.39 it is clearly much more accurate than any other model. Further, 95 percentile ΔE_{ab}^* = 0.87 and maximum ΔE_{ab}^* = 2.28 shows that this model is not only capable to accurately estimate overall response of the device, but also
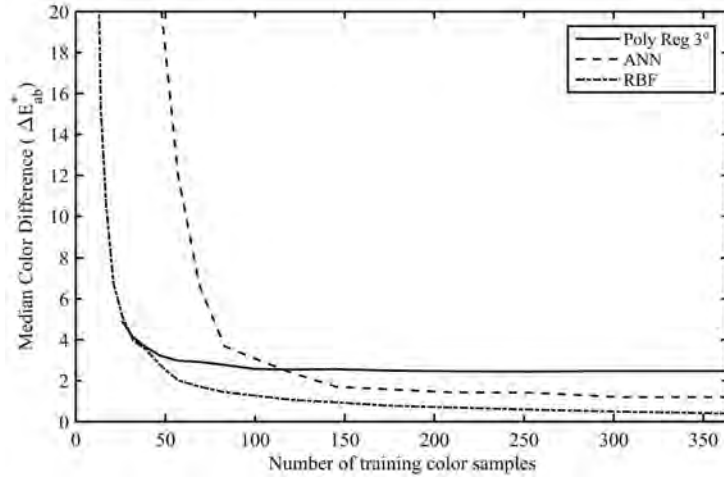
17

Fig. 7: Median ΔE_{ab}^* vs number of training samples. Plot shows that number of training samples have significant impact on the accuracy of all models.
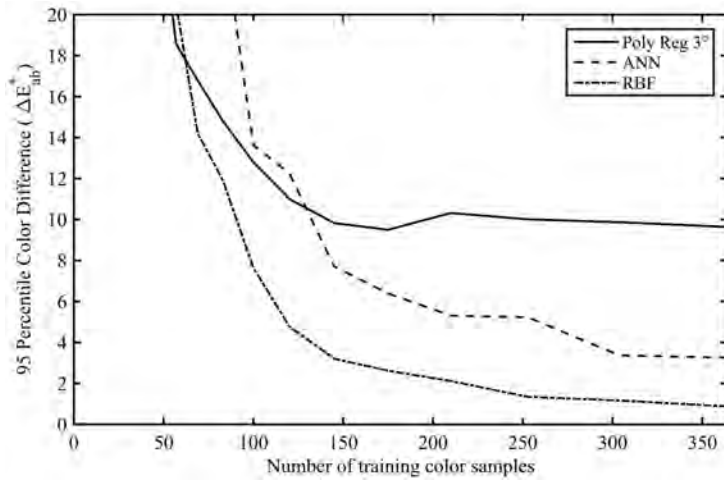
Fig. 8: 95 Percentile ΔE_{ab}^* vs number of training samples. Plot shows that number of training samples have significant impact on the accuracy of all models.

18

Table 1: Comparison of performance of tested models

ΔE_{ab}^*	PLVC	PR 2°	PR 3°	ANN	RBF
Mean	4.17	7.92	3.62	1.62	0.46
Median	4.01	5.31	2.47	1.25	0.39
Std. dev.	2.07	7.08	2.95	1.21	0.26
Min	0.00	1.55	0.71	0.49	0.18
Max	10.63	50.64	19.64	10.35	2.28
95th pctl.	7.93	25.56	9.63	4.46	0.87

estimate response even for colors that are at the boundary of device gamut. This is comparable with the best reported results in [28] of 95 percentile ΔE_{ab}^* = 0.376 and maximum ΔE_{ab}^* = 1.132 for triharmonic kernel (it should be noted here that their results for maximum and 95th percentile ware reported only for one CRT device).

Second best model for characterization of mobile displays is ANN model with median ΔE_{ab}^* = 1.25 This value is still considered to be acceptable for characterization. However, this model have much worse accuracy when it comes to colors at the boundary of gamut with maximum ΔE_{ab}^* = 10.25 and 95 percentile ΔE_{ab}^* = 4.46.

Polynomial regression of second degree is the worst of all tested methods. Even though second degree polynomial in theory can model channel interdependence between any two primaries, in practice this is not enough (median ΔE_{ab}^* = 5.31) since it fails to estimate interdependance of all three primaries, especially on gamut boundary. Polynomial regression of 3rd degree is in that respect better and with acceptable median color difference of 2.47 is among better models. However, with maximum ΔE_{ab}^* = 19.64 it fails when it comes to estimation of colors on gamut boundary. Note that higher degrees of polynomial cannot address this problem. On the contrary, due to Runge's phenomenon, higher order polynomials show even worse results.

19
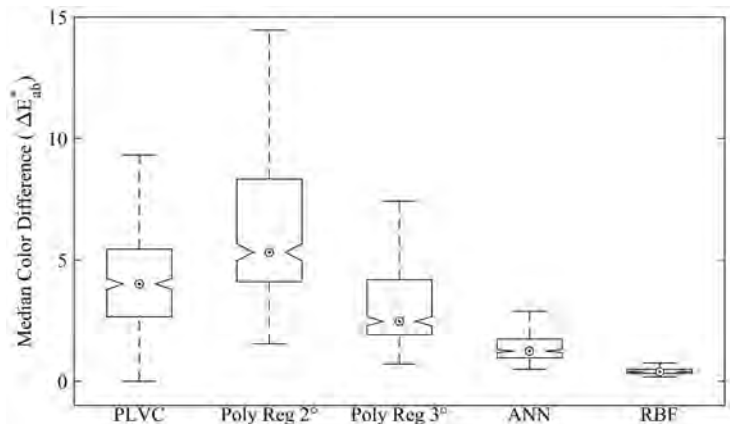
Fig. 9: Performance of tested methods. Boxplot shows that the RBF network model has superior accuracy compared to other models.

Even though PLVC model has somewhat high median color difference (median $\Delta E_{ab}^* = 4.01$) it is actually much better when it comes to overall accuracy, including colors on the gamut boundary (maximum $\Delta E_{ab}^* = 10.63$). With only 27 data points used for characterization it outperforms polynomial regression models. Reason for this is the fact that all 27 data points used belong to pure primaries and combination of pure primaries.

6. Conclusion

In this paper we have implemented and analyzed different models for color characterization of mobile device's display. We have also improved accuracy RBF model by choosing optimal parameters. We conclude that for simple ANN model, the number of neurons in hidden layer is crucial for accuracy of the model. An increase of neurons in the layer improves accuracy. However, after the number of neurons in the hidden layer reaches 17 there is no further improvement.

For proposed RBF model, the accuracy of color characterization can be also optimized by choosing an adequate basis function. The best results were obtained for polyharmonic spline kernel of 4th order.

20

Our investigation of the importance of the size of a training set leads to conclusion that optimum size for ANN and RBF is around 150 samples, while for Polynomial regression models is around 100 samples. Smaller training sets can still lead to models with good average accuracy, but these models will have unacceptable maximum color difference.

Global comparison of all tested models showed that RBF based models have superior performance over other methods. This is especially true for pure primary and secondary colors. This colors are very hard to estimate since they are positioned at the border of device's gamut. Even though RBF using Gaussian or multiquadric functions are worse than RBF with polyharmonic spline they are still better in accuracy than any other tested model, especially for boundary colors. In addition, we can conclude that RBF model with multiquadric function is better option if only a small training set is available.

Future investigation could be focused on distribution of color samples in training set. More extended experiments are needed, but we presume that by carefully choosing color samples used for training, further optimization of a model is possible. Other possible research directions are modification of PLVC model in order to include channel interdependence, or modification of architecture of ANN model to improve its overall accuracy.

References

[1] W. den Boer, Active Matrix Liquid Crystal Displays, Newnes, Burlington.
URL http://www.sciencedirect.com/science/book/9780750678131

[2] C. H. B. Elliott, T. L. Credelle, M. H. Im, P. Higgins, Development of the PenTile Matrix color AMLCD subpixel architecture and rendering algorithms, Journal of SID 11 (1) (2003) 89–98. doi:10.1889/1.1831725.
URL http://www.scopus.com/inward/record.url?eid=2-s2.0-0038004172{&}partnerID=tZOtx3y1

[3] R. S. Berns, Methods for characterizing CRT displays, Displays 16 (4) (1996) 173–182. doi:10.1016/0141-9382(96)01011-6.

21

420   URL `http://linkinghub.elsevier.com/retrieve/pii/0141938296010116`

[4] N. Katoh, T. Deguchi, R. Berns, An Accurate Characterization of CRT Monitor (I) Verifications of Past Studies and Clarifications of Gamma, Optical Review 8 (5) (2001) 305–314. `doi:10.1007/s10043-001-0305-0`.

425   URL `http://dx.doi.org/10.1007/s10043-001-0305-0`

[5] D. L. Post, C. S. Calhoun, Further Evaluation of Methods for Producing Specific Colors on CRT Monitors, Color Research & Application 25 (2) (2000) 90–104. `doi:10.1002/(SICI)1520-6378(200004)25:2<90::AID-COL4>3.0.CO;2-S`.

430   URL `http://onlinelibrary.wiley.com/doi/10.1002/(SICI)1520-6378(200004)25:2<90::AID-COL4>3.0.CO;2-S`

[6] G. Sharma, LCDs versus CRTs-color-calibration and gamut considerations, Proceedings of the IEEE 90 (4) (2002) 605–622. `doi:10.1109/JPROC.2002.1002530`.

435   URL `http://ieeexplore.ieee.org/xpls/abs_all.jsp?arnumber=1002530http://ieeexplore.ieee.org/lpdocs/epic03/wrapper.htm?arnumber=1002530`

[7] E. a. Day, L. Taplin, R. S. Berns, Colorimetric characterization of a computer-controlled liquid crystal display, Color Research & Application 29 (5) (2004) 365–373. `doi:10.1002/col.20046`.

440   URL `http://doi.wiley.com/10.1002/col.20046`

[8] N. Tamura, N. Tsumura, Y. Miyake, Masking model for accurate colorimetric character'ization of LCD, Journal of the Society for Information Display 11 (2) (2003) 333–339. `doi:10.1889/1.1825664`.

445   URL `http://doi.wiley.com/10.1889/1.1828693`

[9] R. Byshko, S. Li, Characterization of iPhone displays: a comparative study, Proceedings of the 18th German Color Group Workshop on Color Image

22

Processing (September) (2012) 49–60.

URL `http://www.hooklee.com/Papers/GCG{_}FarbbildWSS2012.pdf`

[10] N. Ohta, A. Robertson, Colorimetry: fundamentals and applications, John Wiley & Sons, 2005.

[11] J.-B. Thomas, J. Y. Hardeberg, I. Foucherot, P. Gouton, The PLVC display color characterization model revisited, Color Research & Application 33 (6) (2008) 449–460. `doi:10.1002/col.20447`.

URL `http://doi.wiley.com/10.1002/col.20447`

[12] W. B. Cowan, An inexpensive scheme for calibration of a colour monitor in terms of CIE standard coordinates, ACM SIGGRAPH Computer Graphics 17 (3) (1983) 315–321. `doi:10.1145/964967.801163`.

URL `http://portal.acm.org/citation.cfm?doid=964967.801163`

[13] Y. Kwak, L. MacDonald, Characterisation of a desktop LCD projector, Displays 21 (5) (2000) 179–194. `doi:10.1016/S0141-9382(00)00049-4`.

URL `http://www.sciencedirect.com/science/article/pii/S0141938200000494`

[14] Y. Kwak, C. Li, L. MacDonald, Controling color of liquid-crystal displays, Journal of the Society for Information Display 11 (2) (2003) 341. `doi:10.1889/1.1825665`.

URL `http://doi.wiley.com/10.1889/1.1828693`

[15] G. Sharma (Ed.), Digital Color Imaging Handbook, 2nd Edition, CRC Press LCC, Boca Raton, FL, 2002.

[16] A. Neumann, A. Artusi, G. Zotti, L. Neumann, W. Purgathofer, An interactive perception-based model for characterization of display devices, in: R. Eschbach, G. G. Marcu (Eds.), Proceedings of SPIE, Vol. 5293, 2003, pp. 232–241. `doi:10.1117/12.519852`.

URL `http://proceedings.spiedigitallibrary.org/proceeding.aspx?articleid=836901`

23

[17] A. Neumann, A. Artusi, L. Neumann, G. Zotti, W. Purgathofer, Accurate display gamma functions based on human observation, Color Research & Application 32 (4) (2007) 310–319. `doi:10.1002/col.20336`.
URL `http://doi.wiley.com/10.1002/col.20336`

[18] R. S. Berns, M. E. Gorzynski, R. J. Motta, CRT colorimetry. Part II: Metrology, Color Research & Application 18 (5) (1993) 315–325. `doi: 10.1002/col.5080180505`.
URL `http://doi.wiley.com/10.1002/col.5080180505`

[19] R. S. Berns, R. J. Motta, M. E. Gorzynski, CRT colorimetry. part I: Theory and practice, Color Research & Application 18 (5) (1993) 299–314. `doi: 10.1002/col.5080180504`.
URL `http://doi.wiley.com/10.1002/col.5080180504`

[20] D. H. Brainard, Calibration of a computer controlled color monitor, Color Research & Application 14 (1) (1989) 23–34. `doi:10.1002/col. 5080140107`.
URL `http://doi.wiley.com/10.1002/col.5080140107`

[21] N. Katoh, T. Deguchi, R. S. Berns, An Accurate Characterization of CRT Monitor (II) Proposal for an Extension to CIE Method and Its Verification, Optical Review 8 (5) (2001) 397–408. `doi:10.1007/s10043-001-0397-6`.
URL `http://dx.doi.org/10.1007/s10043-001-0397-6http://link.springer.com/10.1007/s10043-001-0397-6`

[22] W. B. Cowan, N. L. Rowell, On the gun independence and phosphor constancy of colour video monitors, Color Research & Applications 11 (11) (1986) S34–S38.

[23] B. Sun, H. Liu, S. Zhou, W. Li, Evaluating the Performance of Polynomial Regression Method with Different Parameters during Color Characterization, Mathematical Problems in Engineering 2014 (3) (2014) 1–7. `doi:10.1155/2014/418651`.
URL `http://www.hindawi.com/journals/mpe/2014/418651/`

24

[24] M. Luo, Device calibration of a color image scanner digitizing system by using neural networks, in: Proceedings of ICNN'95 - International Conference on Neural Networks, Vol. 1, IEEE, 1995, pp. 59–62. `doi:10.1109/ICNN.1995.487877`.
URL `http://ieeexplore.ieee.org/lpdocs/epic03/wrapper.htm?arnumber=487877`

[25] S. Usui, Y. Arai, S. Nakauchi, Neural networks for device-independent digital color imaging, Information Sciences 123 (1-2) (2000) 115–125. `doi:10.1016/S0020-0255(99)00113-9`.
URL `http://linkinghub.elsevier.com/retrieve/pii/S0020025599001139http://www.sciencedirect.com/science/article/pii/S0020025599001139`

[26] J. Z. Chan, J. P. Allebach, C. A. Bouman, Sequential linear interpolation of multidimensional functions., IEEE transactions on image processing : a publication of the IEEE Signal Processing Society 6 (9) (1997) 1231–45. `doi:10.1109/83.623187`.
URL `http://www.ncbi.nlm.nih.gov/pubmed/18283013`

[27] G. Sharma, M. Shaw, Thin-plate splines for printer data interpolation, in: 14th European Signal Processing Conference (EUSIPCO 2006), IEEE, Florence, Italy, 2006, pp. 1–5.
URL `http://ieeexplore.ieee.org/xpls/abs_all.jsp?arnumber=7071774&tag=1`

[28] P. Colantoni, J.-b. Thomas, J. Y. Hardeberg, High-end colorimetric display characterization using an adaptive training set, Journal of the Society for Information Display 19 (8) (2011) 520. `doi:10.1889/JSID19.8.520`.
URL `http://doi.wiley.com/10.1889/1.1828693`

[29] A. Artusi, Novel color printer characterization model, Journal of Electronic Imaging 12 (3) (2003) 448. `doi:10.1117/1.1579016`.

URL http://electronicimaging.spiedigitallibrary.org/article.aspx?doi=10.1117/1.1579016

[30] B. Bastani, B. Cressman, B. Funt, Calibrated color mapping between LCD and CRT displays: A case study, Color Research & Application 30 (6) (2005) 438–447. doi:10.1002/col.20156.
URL http://doi.wiley.com/10.1002/col.20156

[31] I. Amidror, Scattered data interpolation methods for electronic imaging systems: a survey, Journal of Electronic Imaging 11 (2) (2002) 157. doi:10.1117/1.1455013.
URL http://electronicimaging.spiedigitallibrary.org/article.aspx?doi=10.1117/1.1455013

[32] W. W. Farley, J. C. Gutmann, Digital image processing systems and an approach to the display of colors of specified chrominance, Tech. rep., Blacksburg (1980).

[33] D. L. Post, C. S. Calhoun, An evaluation of methods for producing desired colors on CRT monitors, Color Research & Application 14 (4) (1989) 172–186. doi:10.1002/col.5080140406.
URL http://doi.wiley.com/10.1002/col.5080140406

[34] N. Tamura, N. Tsumura, Y. Miyake, Masking model for accurate colorimetric characterization of LCD, Journal of the Society for Information Display 11 (2) (2003) 333. doi:10.1889/1.1825664.
URL http://doi.wiley.com/10.1889/1.1828693

[35] L. D. Jiménez Barco, J. a. Díaz, J. R. Jiménez, M. Rubiño, Considerations on the calibration of color displays assuming constant channel chromaticity, Color Research & Application 20 (6) (1995) 377–387. doi:10.1002/col.5080200606.
URL http://doi.wiley.com/10.1002/col.5080200606

[36] B. Schölkopf, A. J. Smola, Learning with kernels: support vector machines, regularization, optimization, and beyond, 2nd Edition, MIT press, 2002.

[37] K.-A. Toh, W.-Y. Yau, X. Jiang, A Reduced Multivariate Polynomial Model for Multimodal Biometrics and Classifiers Fusion, IEEE Transactions on Circuits and Systems for Video Technology 14 (2) (2004) 224–233. `doi:10.1109/TCSVT.2003.821974`.
URL `http://ieeexplore.ieee.org/lpdocs/epic03/wrapper.htm?arnumber=1269755`

[38] D. Donevski, D. Milcic, D. Banic, Effect of data scaling on color device model fitting, Journal of Industrial Engineering and Management 3 (2) (2010) 399–407. `doi:10.3926/jiem.2010.v3n2.p399-407`.
URL `http://jiem.org/index.php/jiem/article/view/271`

[39] M. Xia, E. Saber, G. Sharma, a. M. Tekalp, End-to-end color printer calibration by total least squares regression, IEEE transactions on image processing : a publication of the IEEE Signal Processing Society 8 (5) (1999) 700–16. `doi:10.1109/83.760337`.
URL `http://www.ncbi.nlm.nih.gov/pubmed/18267485`

[40] M. P. Allen, Understanding Regression Analysis, Springer US, Boston, MA, 1997. `doi:10.1007/b102242`.
URL `http://link.springer.com/10.1007/b102242`

[41] H. R. Kang, Computational color technology, SPIE The International Society for Optical Engineering, Bellingham, 2006.
URL `http://spie.org/x648.html?product_id=660835`

[42] G. Zhang, Neural networks for classification: a survey, IEEE Transactions on Systems, Man and Cybernetics, Part C (Applications and Reviews) 30 (4) (2000) 451–462. `doi:10.1109/5326.897072`.
URL `http://ieeexplore.ieee.org/lpdocs/epic03/wrapper.htm?arnumber=897072`

27

[43] F. Scarselli, A. Chung Tsoi, Universal Approximation Using Feed-forward Neural Networks: A Survey of Some Existing Methods, and Some New Results, Neural Networks 11 (1) (1998) 15–37. `doi:10.1016/S0893-6080(97)00097-X`.
URL `http://www.ncbi.nlm.nih.gov/pubmed/12662846http://linkinghub.elsevier.com/retrieve/pii/S089360809700097X`

[44] K. Hornik, Approximation Capabilities of Multilayer Feedforward Networks, Neural Networks 4 (2) (1991) 251–257. `doi:10.1016/0893-6080(91)90009-T`.
URL `http://dx.doi.org/10.1016/0893-6080(91)90009-T`

[45] S. Chen, C. N. Cowan, P. M. Grant, Orthogonal least squares learning algorithm for radial basis function networks., IEEE transactions on neural networks / a publication of the IEEE Neural Networks Council 2 (2) (1991) 302–9. `doi:10.1109/72.80341`.
URL `http://www.ncbi.nlm.nih.gov/pubmed/18276384`

[46] G. Lera, M. Pinzolas, Neighborhood based Levenberg-Marquardt algorithm for neural network training, IEEE Transactions on Neural Networks 13 (5) (2002) 1200–1203. `doi:10.1109/TNN.2002.1031951`.

[47] R. L. Hardy, Multiquadric equations of topography and other irregular surfaces, Journal of Geophysical Research 76 (8) (1971) 1905–1915. `doi:10.1029/JB076i008p01905`.
URL `http://doi.wiley.com/10.1029/JB076i008p01905`

[48] R. Hardy, Theory and applications of the multiquadric-biharmonic method 20 years of discovery 19681988, Computers & Mathematics with Applications 19 (8-9) (1990) 163–208. `doi:10.1016/0898-1221(90)90272-L`.
URL `http://linkinghub.elsevier.com/retrieve/pii/089812219090272L`

[49] H. Rocha, On the selection of the most adequate radial basis function, Applied Mathematical Modelling 33 (3) (2009) 1573–1583.

28

doi:10.1016/j.apm.2008.02.008.

URL   `http://linkinghub.elsevier.com/retrieve/pii/`
`S0307904X08000590`

[50] J. Schanda, CIE Colorimetry, in: J. Schanda (Ed.), Coloimetry: Understanding the CIE system, John Wiley & Sons, 2007, pp. 29–82.